Electronic Supplementary Material (ESI) for Physical Chemistry Chemical Physics.

Electronic Supporting Information: Ultrafast Charge Transfer in a Nonfullerene All-Small-Molecule Organic Solar Cell: A Nonadiabatic Dynamics Simulation with Optimally Tuned Range-Separated Functional

Dan Mao[1], Xin-Rui Chen[1], Dong-Heng Li[1], Xiang-Yang Liu[1],* Ganglong Cui[2], and Laicai Li[1]*

[1]*College of Chemistry and Material Science, Sichuan Normal University, Chengdu 610068, China and* [2]*Key Laboratory of Theoretical and Computational Photochemistry, Ministry of Education, College of Chemistry, Beijing Normal University, Beijing 100875, China*

E-mail: xiangyangliu@sicnu.edu.cn; lilcmail@163.com

Methods

Semi-Classical Absorption Spectra Simulation

Absorption spectra are simulated with a semi-classical method proposed by Barbatti et al.[1,2] On the basis of ground-state ensembles composed of N structures $\mathbf{R}_k$, we can calculate photoabsorption cross section with time-dependent perturbation theory at the first-order level

$$\sigma(E) = \frac{\pi e^2}{2mc\varepsilon_0} \sum_{l \neq i} \left[\frac{1}{N} \sum_{k}^{N} f_{il}(\mathbf{R}_k)\, g\left(E - \Delta E_{il}(\mathbf{R}_k), \delta\right) \right] \tag{S1}$$

where ε_0 is vacuum dielectric constant; c is speed of light; e and m are electron charge and mass; $f_{il}(\mathbf{R}_k)$ and $\Delta E_{il}(\mathbf{R}_k)$ are oscillator strength and transition energy from initial i to final l state at structure $\mathbf{R}_k$; $g\left(E - \Delta E_{il}(\mathbf{R}_k), \delta\right)$ is a normalized line shape function that is peaked at transition energy $\Delta E_{il}(\mathbf{R}_k)$ and broadened by a phenomenological constant δ. In practical applications, there are two kinds of shape functions used to model line shapes. The first one is Gaussian shape function

$$g_{Gauss}(E - \Delta E_{il}, \delta) = \left(\frac{2}{\pi}\right)^{1/2} \frac{\hbar}{\delta} exp\left(\frac{-2\left(E - \Delta E_{il}\right)^2}{\delta^2}\right) \tag{S2}$$

the second one is Lorentzian shape function

$$g_{Lorentz}(E - \Delta E_{il}, \delta) = \frac{\hbar\delta}{2\pi} \left[\left(E - \Delta E_{il}\right)^2 + \left(\frac{\delta}{2}\right)^2 \right]^{-1} \tag{S3}$$

in which $\hbar$ is reduced Planck constant. Our group has recently implemented this method for absorption spectra simulations.[3–6] In the present work, Gaussian shape function is used for simulating absorption spectra from ground to excited state ($i = 0$).

Fewest-Switches Surface-Hopping Method

The trajectory-based fewest-switches surface-hopping dynamics simulation approaches by Tully et al.[7] has been extensively employed to simulate a variety of ultrafast excited-state relaxation processes in chemical/biological systems and materials.[8–16] In the following, a brief presentation is given.

Treating nuclear coordinates $\mathbf{R}(t)$ as variables, the time-dependent electronic Schrödinger equation can be written as

$$i\hbar\dot{\Psi}(\mathbf{r}, \mathbf{R}(t), t) = \hat{H}_0(\mathbf{r}, \mathbf{R}(t))\Psi(\mathbf{r}, \mathbf{R}(t), t) \tag{S4}$$

where $\hat{H}_0(\mathbf{r}, \mathbf{R}(t))$ is the zero-order electronic Hamiltonian while $\mathbf{r}$ represents the electronic coordinates. The time-dependent electronic wavefunction is then expressed in terms of a linear combination

of adiabatic zero-order electronic spatial wavefunctions:

$$\Psi(\mathbf{r}, \mathbf{R}(t), t) = \sum_{i=1}^{N} C_i(t)\Psi_i(\mathbf{r}, \mathbf{R}(t)) \tag{S5}$$

in which $\Psi_i(\mathbf{r}, \mathbf{R}(t))$ is an eigenfunction of zero-order Hamiltonian $\hat{H}_0(\mathbf{r}, \mathbf{R}(t))$ at nuclear coordinates $\mathbf{R}(t)$. Substituting Eq. S5 into Eq. S4, multiplying by $\Psi_j^*(\mathbf{r}, \mathbf{R}(t))$ and integrating over the electronic coordinates, we obtain

$$\dot{C}_j(t) = -i\hbar^{-1}C_j(t)E_j(\mathbf{R}(t)) - \sum_{i}^{N} C_i(t)\tau_{ji}(t) \tag{S6}$$

where $\tau_{ji}(t) = \langle\Psi_j|\frac{\partial}{\partial t}\Psi_i\rangle$ is the time derivative nonadiabatic coupling between adiabatic states i and j. $\tau_{ji}(t)$ can also be expressed as $\mathbf{v}(t) \cdot \mathbf{d}_{ji}(\mathbf{R}(t))$ in which $\mathbf{v}(t)$ and $\mathbf{d}_{ji}(\mathbf{R}(t))$ are the nuclear velocities and the adiabatic derivative couplings, respectively. Thus, Eq. S6 can also be written as

$$\dot{C}_j(t) = -i\hbar^{-1}C_j(t)E_j^0(\mathbf{R}(t)) - \sum_{i}^{N} C_i(t)\mathbf{v}(t) \cdot \mathbf{d}_{ji}(\mathbf{R}(t)) \tag{S7}$$

which is the central equation of the fewest-switches surface-hopping method and may describe radiationless transitions between electronic states with the same spin. The fewest-switches criterion finally yields the transition probability from state i to j as

$$p_{ij}(t)dt = 2\frac{\mathrm{Re}(C_i^* C_j \tau_{ij})}{C_i^* C_i}dt \tag{S8}$$

This method has been implemented in our own GTSH package[17] and widely used to simulation photoinduced ultrafast processes of molecular, biological and materials systems.[18–23]

Time-Derivative Nonadiabatic Couplings

The time derivative nonadiabatic couplings $\tau_{ji}(t)$ can be calculated from the adiabatic derivative couplings $\mathbf{d}_{ji}(\mathbf{R}(t))$ and the nuclear velocities $\mathbf{v}(t)$, and there are also some analytical expressions for

$\mathbf{d}_{ji}(\mathbf{R}(t))$.[24–26] In addition, there are two types of numerical algorithms available to directly compute $\tau_{ji}(t)$ in the framework of LR-TDDFT.[27,28] Our present work uses the recently developed algorithm. A brief presentation is given below, in which the subscripts $\{a, b, c\}$ denote the virtual orbitals, $\{i, j, k\}$ the occupied orbitals, and $\{p, q, r\}$ for any type of orbitals.

In LR-TDDFT the total electronic wave function of an electronically excited state Ψ_K is approximately written as a linear combination of singly-excited Slater determinants,

$$\Psi_K = \sum_{i}^{occ} \sum_{a}^{unocc} w_{ia}^{K} \psi_i^a \tag{S9}$$

in which w_{ia}^K is the coefficient of the singly-excited Slater determinant ψ_i^a. The determinant $\psi_i^a = \hat{a}_a^\dagger \hat{a}_i \psi_0$ is constructed through the electronic excitation (substitution) operation of the ground-state determinant ψ_0. Thereby, the time derivative nonadiabatic coupling $\tau_{KJ} = \langle \Psi_K | \frac{\partial}{\partial t} \Psi_J \rangle$, can be further written as

$$\tau_{KJ} = \sum_{ijab} \left(w_{ia}^{K*} \partial_t w_{jb}^{J} \left\langle \psi_i^a \middle| \psi_j^b \right\rangle + w_{ia}^{K*} w_{jb}^{J} \left\langle \psi_i^a \middle| \partial_t \psi_j^b \right\rangle \right) \tag{S10}$$

The first term simplifies to $\sum_{ia} w_{ia}^{K*} \partial_t w_{ia}^{J}$ due to the orthogonality condition for the molecular orbitals (MOs) $\langle \phi_p | \phi_q \rangle = \delta_{pq}$. The time differentiation on ψ_j^b gives

$$\partial_t \psi_j^b = \sum_{k \neq j} \psi_j^b \{k\}' + \psi_j^{b'} \tag{S11}$$

where $\psi_p^q \{r\}'$ denotes a determinant originated from ψ_p^q but with the MO ϕ_r ($r \neq p$) replaced by its time derivative $\partial_t \phi_r$, and $\psi_p^{q'}$ denotes a determinant originated from ψ_p^q but with the MO ϕ_p replaced by the time derivative $\partial_t \phi_q$. Therefore, the 2nd term in formula S10 becomes

$$\left\langle \psi_i^a \middle| \partial_t \psi_j^b \right\rangle = \sum_{k \neq j} \left\langle \psi_i^a \middle| \psi_{jk}^{bk'} \right\rangle + \left\langle \psi_i^a \middle| \psi_j^{b'} \right\rangle \tag{S12}$$

in which the last term above is reduced to $\delta_{ij} \langle \phi_a | \partial_t \phi_b \rangle$, while only one term with $k = i$ and $a = b$ from sum over k survives due to orthogonality conditions ($\langle \phi_p | \partial_t \phi_p \rangle = 0$ for real orbitals; $\langle \phi_p | \phi_q \rangle = \delta_{pq}$).

Then, we arrive at

$$\left\langle \psi_i^a \left| \partial_t \psi_j^b \right. \right\rangle = \delta_{ij} \left\langle \phi_a \left| \partial_t \phi_b \right. \right\rangle - P_{ij} \delta_{ab} \left\langle \phi_j \left| \partial_t \phi_i \right. \right\rangle \tag{S13}$$

where P_{ij} is an additional phase factor that depends on the ordering convention for the orbitals used in the Slater determinants.

Finally, the computational expression for the time derivative nonadiabatic couplings is written as

$$\tau_{KJ} = \sum_{ia} w_{ia}^K \partial_t w_{ia}^J + \sum_{iab} w_{ia}^K w_{ib}^J \left\langle \phi_a \left| \partial_t \phi_b \right. \right\rangle - \sum_{ija} P_{ij} w_{ia}^K w_{ja}^J \left\langle \phi_j \left| \partial_t \phi_i \right. \right\rangle \tag{S14}$$

in which the terms related to the time derivatives of MOs can be calculated using a finite-difference scheme

$$\left\langle \phi_p \left| \partial_t \phi_q \right. \right\rangle = \frac{1}{\Delta t} \left\langle \phi_p \left(t \right) \left| \phi_q \left(t + \Delta t \right) \right. \right\rangle \tag{S15}$$

where $\phi_p \left(t \right)$ and $\phi_q \left(t + \Delta t \right)$ represent MOs at t and $t + \Delta t$ times, respectively. The corresponding algorithm has been independently coded into a standalone module in our developed GTSH package.[4–6]

Fragment-Based Exciton Analysis

There are several analysis methods capable of examining the excited-state characters, intra- and intermolecular electron and energy transfers of complex systems and in particular the donor–acceptor systems. One of the most popular methods is based on analyzing one-electron transition density matrices, which can be implemented in different atomic orbital representations, e.g. nonorthogonal atomic orbitals[29] or Löwdin orthogonalized atomic orbitals.[30] Recently we have implemented a similar analysis method using Löwdin orthogonalized atomic orbital representation.[3] Within such, the one-electron transition density matrix $\mathbf{T}_{LO}$ is expressed as

$$\mathbf{T}_{\mathrm{LO}} = \left(\mathbf{S}_{\mathrm{AO}} \right)^{1/2} \mathbf{T}_{\mathrm{AO}} \left(\mathbf{S}_{\mathrm{AO}} \right)^{1/2} = \left(\mathbf{S}_{\mathrm{AO}} \right)^{1/2} \left(\mathbf{C} \mathbf{T}_{\mathrm{MO}} \mathbf{C}^{\mathrm{T}} \right) \left(\mathbf{S}_{\mathrm{AO}} \right)^{1/2} \tag{S16}$$

where $\mathbf{C}$ and $\mathbf{S}_{AO}$ are the MO coefficients and AO overlap matrices, and $\mathbf{T}_{AO}$ and $\mathbf{T}_{MO}$ represent the one-electron transition density matrices in the AO and MO representations, respectively. Due to the

orthogonal property of Löwdin atomic orbitals, the transition contribution from atom a to b becomes

$$D_{ab} = \sum_{i \in a, j \in b} (\mathbf{T}_{\mathrm{LO}})_{ij}^2 \tag{S17}$$

where i and j are the indices of the atomic orbitals, and a and b are the indices of the atoms. Thus, transition contribution from a fragment D to another fragment A in a system is given by

$$\Omega_{DA} = \sum_{a \in D, b \in A} D_{ab} \tag{S18}$$

in which $D = A$ and $D \neq A$ represent the local excitation (LE) within fragment D and the charge transfer (CT) excitation from D to A, respectively. Accordingly, contributions of LE and CT to an excited state of interest can be quantitatively obtained. These Ω_{DA} can also be regarded as weights of different fragment-based LE and CT excitons. Moreover, time-dependent electron and hole counts on a fragment can also be calculated.[4–6] The hole count on a fragment D, as a result of electron transfer from D to all fragments A, is computed as

$$h_D = \sum_{a \in D} D_{ab} = \sum_{A} \Omega_{DA} \tag{S19}$$

while, the electron count of a fragment A transferred from all fragments D is defined as

$$e_A = \sum_{b \in A} D_{ab} = \sum_{D} \Omega_{DA} \tag{S20}$$

Electron-Hole Density

Electronic excitation always results in many pairs of hole and electron, which are represented as singly excited Slater determinants ψ_i^a in LR-TDDFT calculations (see above). These electron-hole pairs can be described by occupied and unoccupied MO indices. However, such kind of analysis could be complex if many pairs of MOs are involved. Instead, analyzing spatial distribution of electron and hole produced by all pairs of involved MOs is more useful. In such scheme, hole and electron densities are written as follows[31,32]

$$\rho^{hole}(\mathbf{r}) = \rho^{hole}_{loc}(\mathbf{r}) + \rho^{hole}_{cross}(\mathbf{r}) = \sum_{i\to a}(w_{ia})^2 \phi_i(\mathbf{r})\phi_i(\mathbf{r}) + \sum_{i\to a}\sum_{j\neq i\to a} w_{ia}w_{ja}\phi_i(\mathbf{r})\phi_j(\mathbf{r}) \quad \text{(S21)}$$

$$\rho^{electron}(\mathbf{r}) = \rho^{electron}_{loc}(\mathbf{r}) + \rho^{electron}_{cross}(\mathbf{r}) = \sum_{i\to a}(w_{ia})^2 \phi_a(\mathbf{r})\phi_a(\mathbf{r}) + \sum_{i\to a}\sum_{i\to b\neq a} w_{ia}w_{ib}\phi_a(\mathbf{r})\phi_b(\mathbf{r}) \quad \text{(S22)}$$

in which $\sum_{i\to a} \equiv \sum_i^{occ}\sum_a^{vir}$ and $\sum_{i\to a}\sum_{j\neq i\to a} \equiv \sum_i^{occ}\sum_{j\neq i}^{occ}\sum_a^{vir}$; w_{ia} is coefficient of excited Slater determinant ψ_i^a in an electronically excited electronic state; $\phi_i(\mathbf{r})$ and $\phi_j(\mathbf{r})$ are MOs that hole occupies; $\phi_a(\mathbf{r})$ and $\phi_b(\mathbf{r})$ are MOs that electron occupies. In these equations, the first and second terms stand for contributions of local and cross terms. It is clear that these two electron and hole densities satisfy $\int \rho^{hole}(\mathbf{r})\,d\mathbf{r} = 1$ and $\int \rho^{electron}(\mathbf{r})\,d\mathbf{r} = 1$ due to orthonormality properties of MOs and total sum of squares of all configuration coefficients is 1.0, which means that only one electron is excited leaving one hole. On the basis of electron and hole densities, useful parameters to characterize electron–hole separation can be defined, such as distance of centroids of electron and hole.

Based on density distributions of hole and electron, centroids of hole and electron can be calculated to approximately represent positions of hole and electron. In such case, centroid coordinates X, Y, and Z of electron can be calculated as

$$X_{electron} = \int x\rho^{electron}(\mathbf{r})\,d\mathbf{r} \quad \text{(S23)}$$

$$Y_{electron} = \int y\rho^{electron}(\mathbf{r})\,d\mathbf{r} \quad \text{(S24)}$$

$$Z_{electron} = \int z\rho^{electron}(\mathbf{r})\,d\mathbf{r} \quad \text{(S25)}$$

where x, y, and z are Cartesian coordinate components of electron. Similarly, one can define those for

hole.

Additional Figures and Table

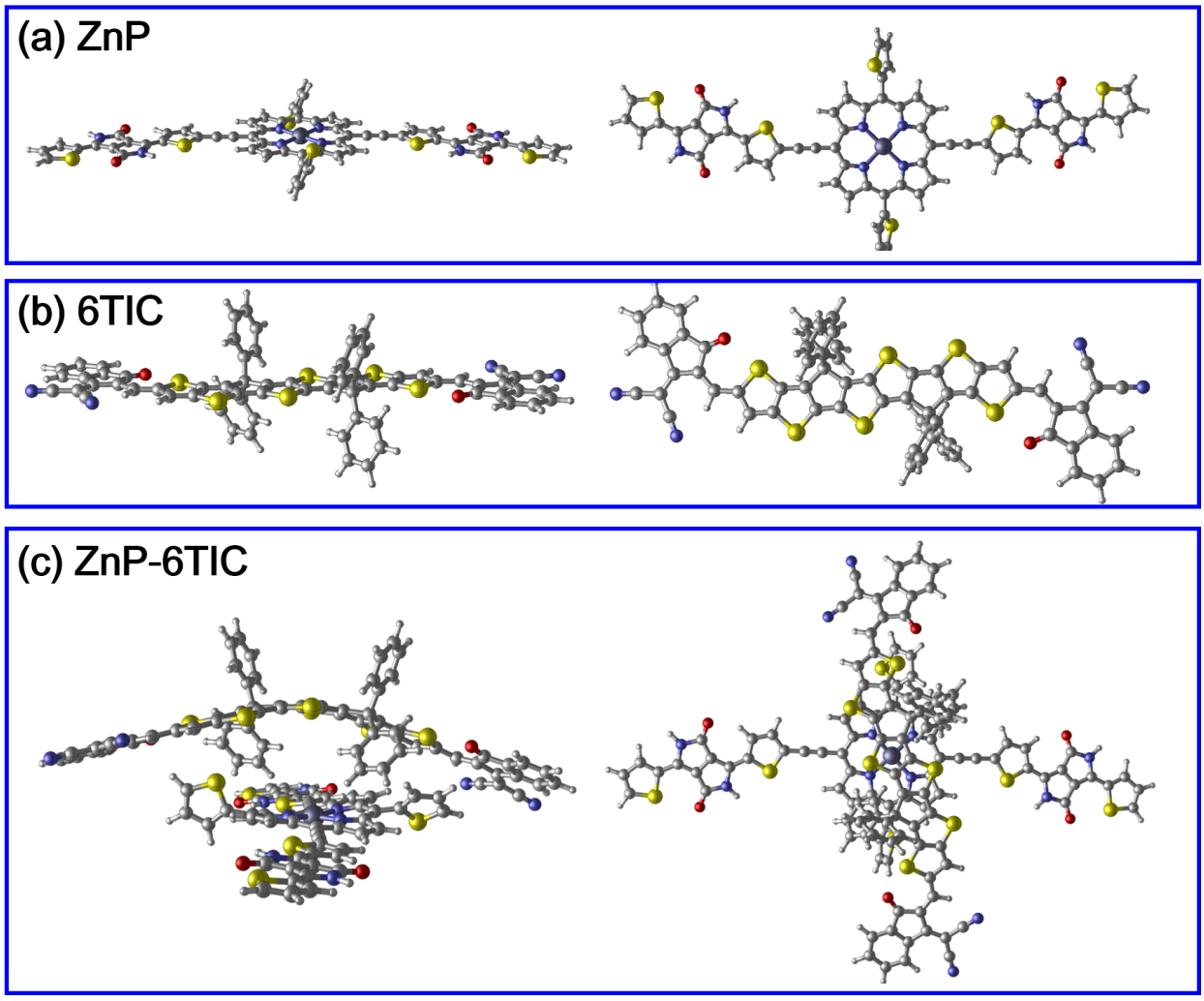

Figure S1: The side view (left) and top view (right) of the ZnP (a), 6TIC (b) and ZnP-6TIC in perpendicular conformation (c) structures optimized at PBE+D3 level.

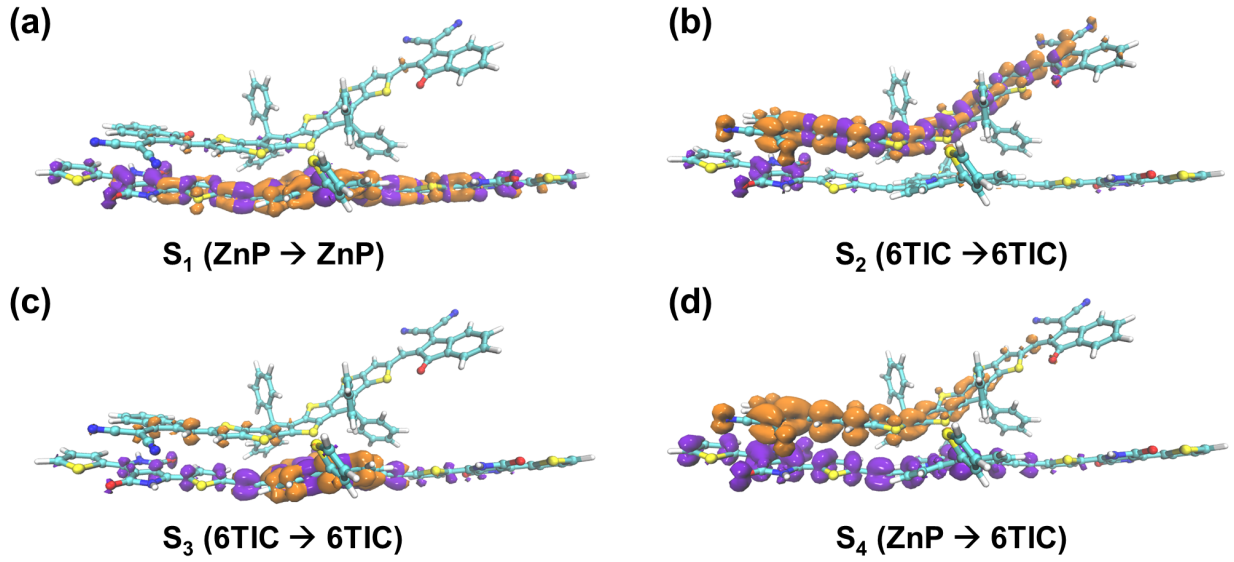

Figure S2: TD-CAM-B3LYP calculated photoinduced electron (in orange) and hole (in purple) densities of the lowest four singlet excited states of ZnP-6TIC. Also shown are their corresponding electronic structure characteristics roughly assigned according to their spatial distributions of electron and hole densities.

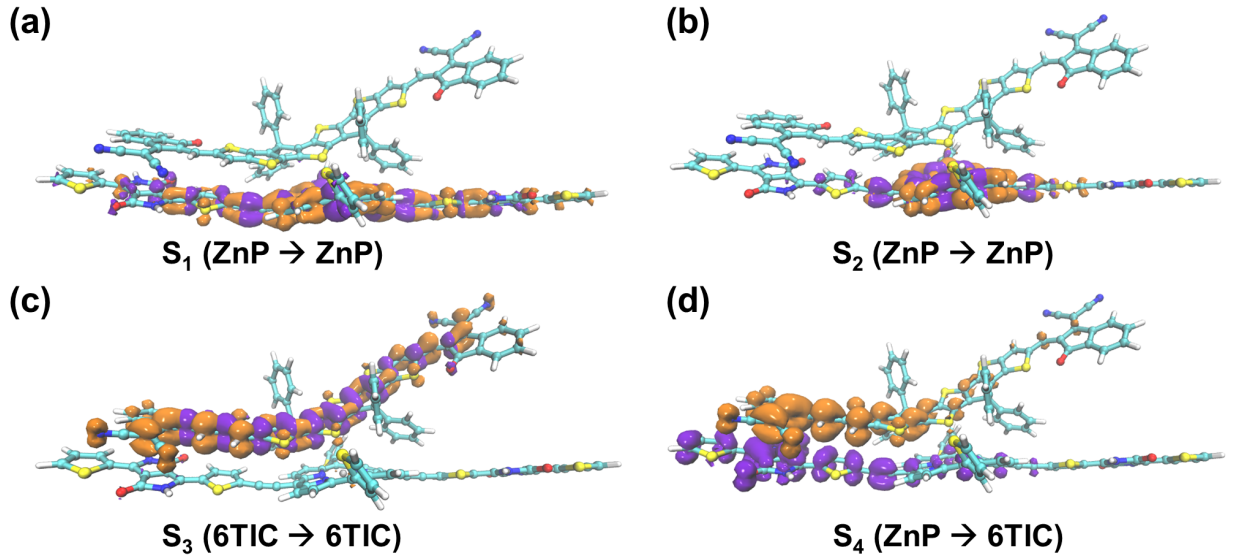

Figure S3: TD-ωB97XD calculated photoinduced electron (in orange) and hole (in purple) densities of the lowest four singlet excited states of ZnP-6TIC. Also shown are their corresponding electronic structure characteristics roughly assigned according to their spatial distributions of electron and hole densities.

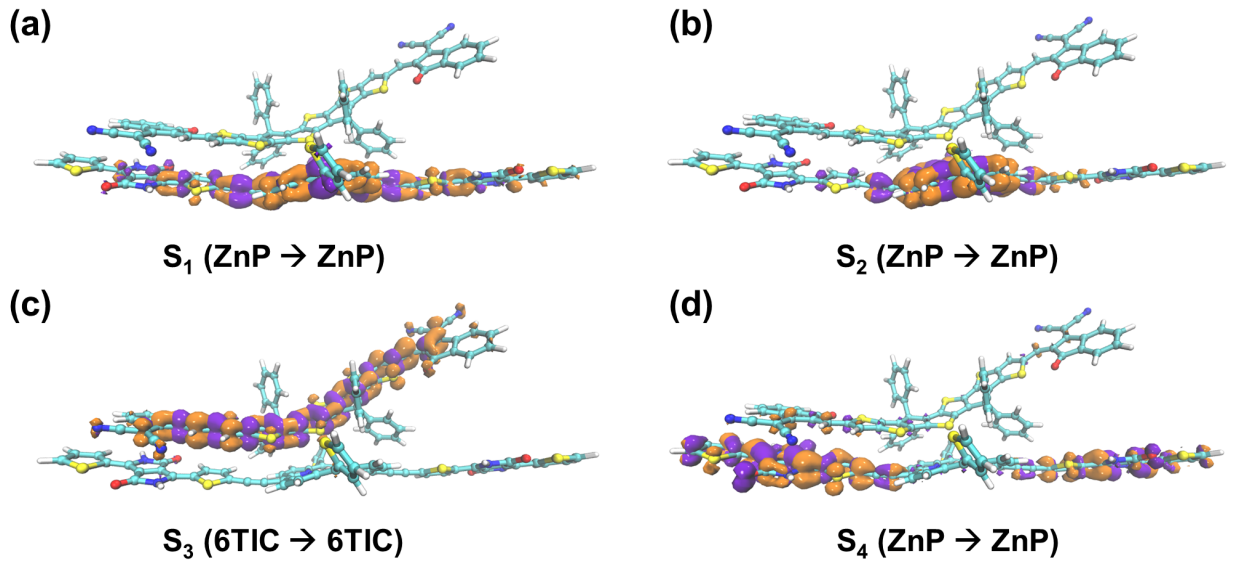

Figure S4: TD-LC-PBE0 calculated photoinduced electron (in orange) and hole (in purple) densities of the lowest four singlet excited states of ZnP-6TIC. Also shown are their corresponding electronic structure characteristics roughly assigned according to their spatial distributions of electron and hole densities.

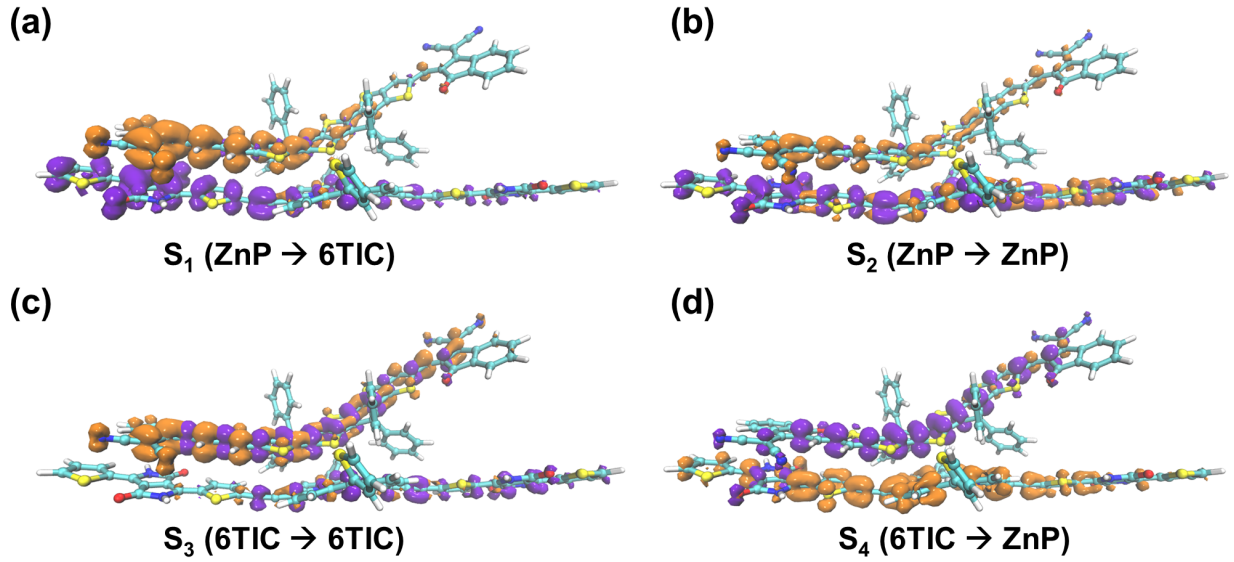

Figure S5: TD-ωB97XD* calculated photoinduced electron (in orange) and hole (in purple) densities of the lowest four singlet excited states of ZnP-6TIC. Also shown are their corresponding electronic structure characteristics roughly assigned according to their spatial distributions of electron and hole densities.

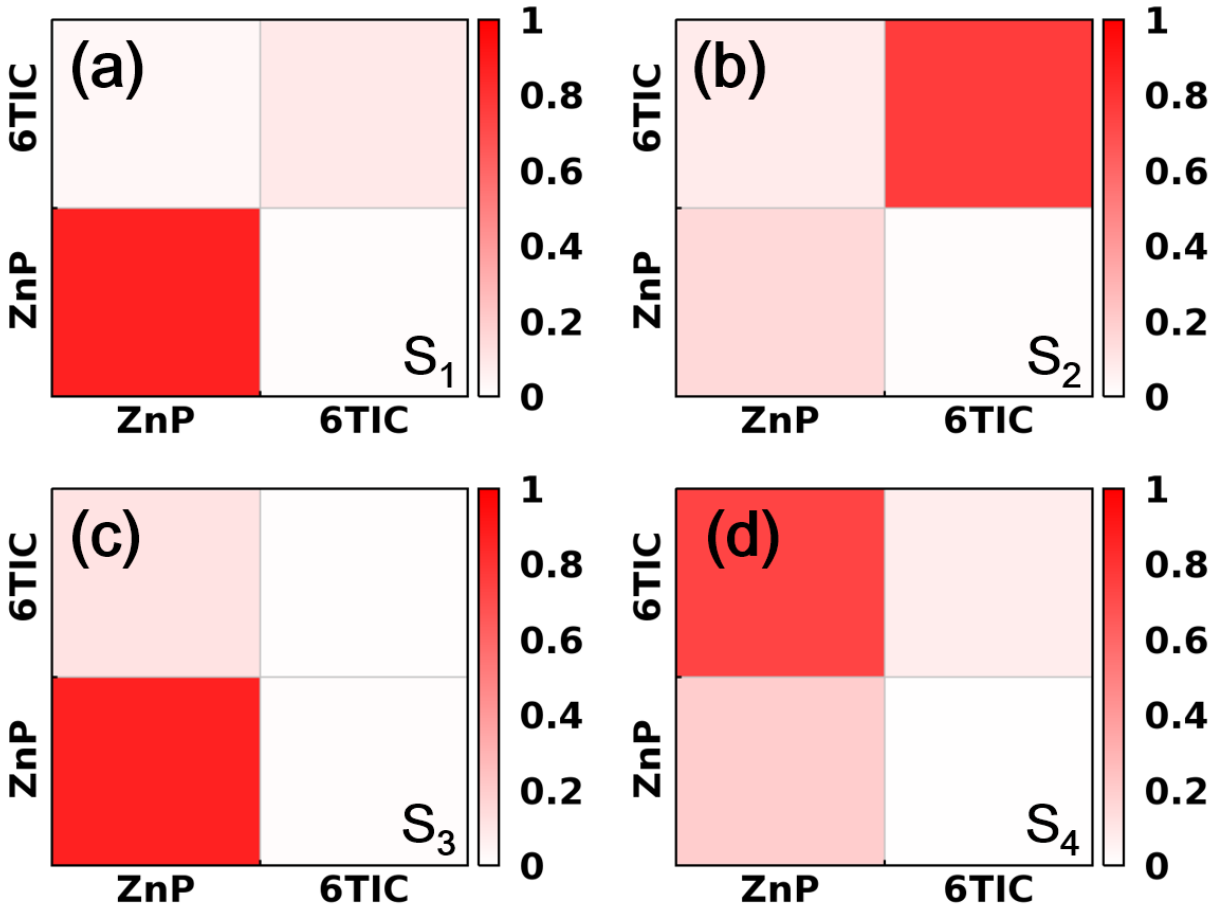

Figure S6: TD-CAM-B3LYP calculated one-electron transition density matrices (1TDM) for the lowest four excited states of Franck-Condon point ZnP-6TIC, where the X-axis represents the donor ZnP fragment and the Y-axis represents the acceptor 6TIC fragment.

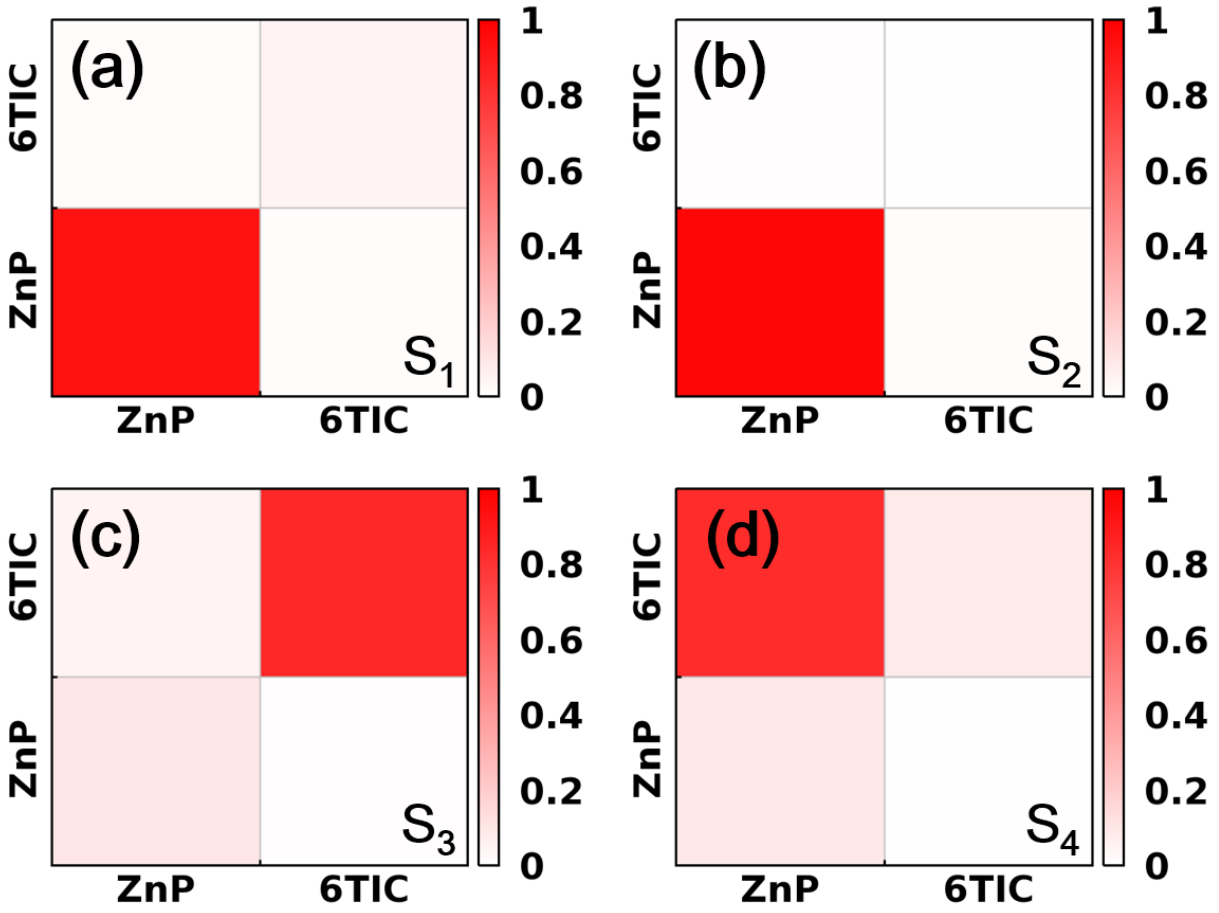

Figure S7: TD-ωB97XD calculated one-electron transition density matrices (1TDM) for the lowest four excited states of Franck-Condon point ZnP-6TIC, where the X-axis represents the donor ZnP fragment and the Y-axis represents the acceptor 6TIC fragment.

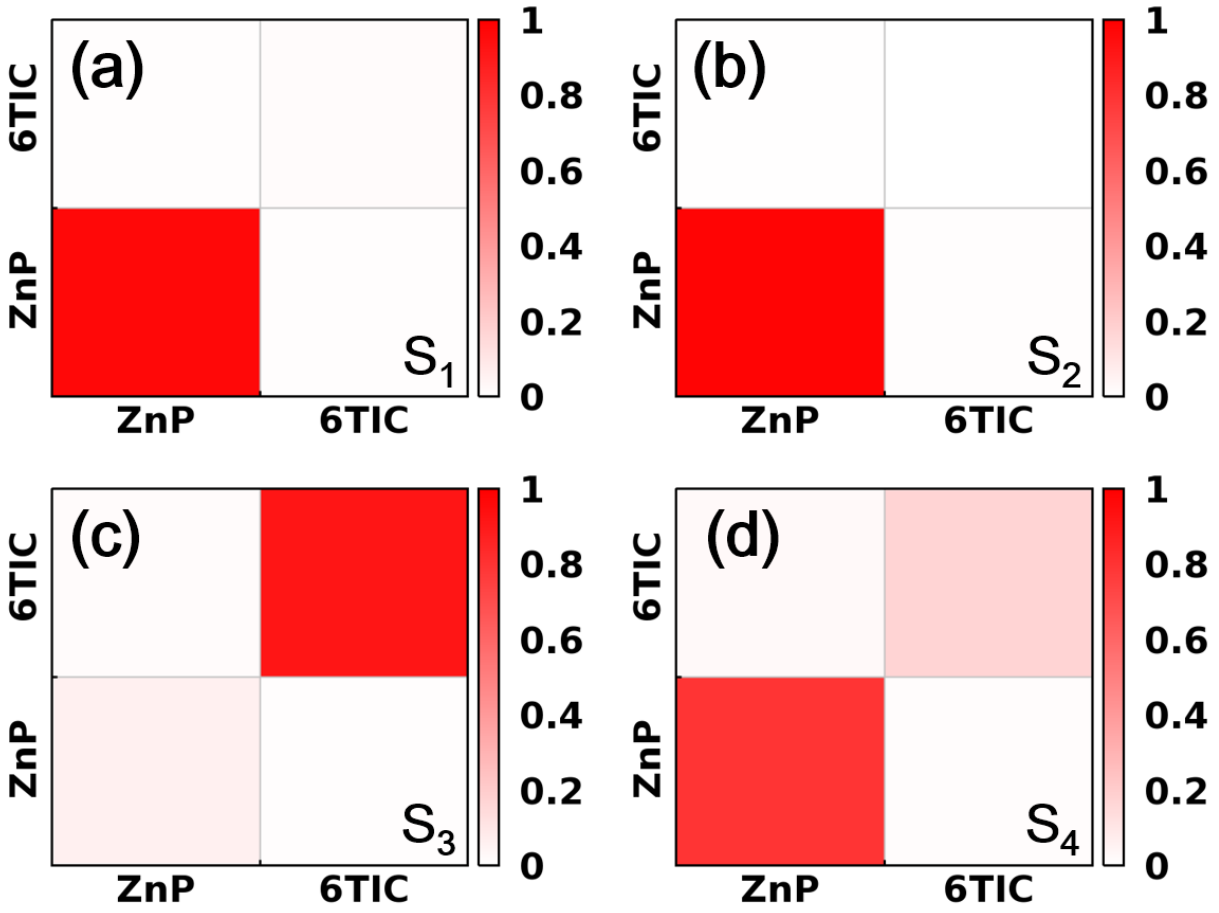

Figure S8: TD-LC-PBE0 calculated one-electron transition density matrices (1TDM) for the lowest four excited states of Franck-Condon point ZnP-6TIC, where the X-axis represents the donor ZnP fragment and the Y-axis represents the acceptor 6TIC fragment.

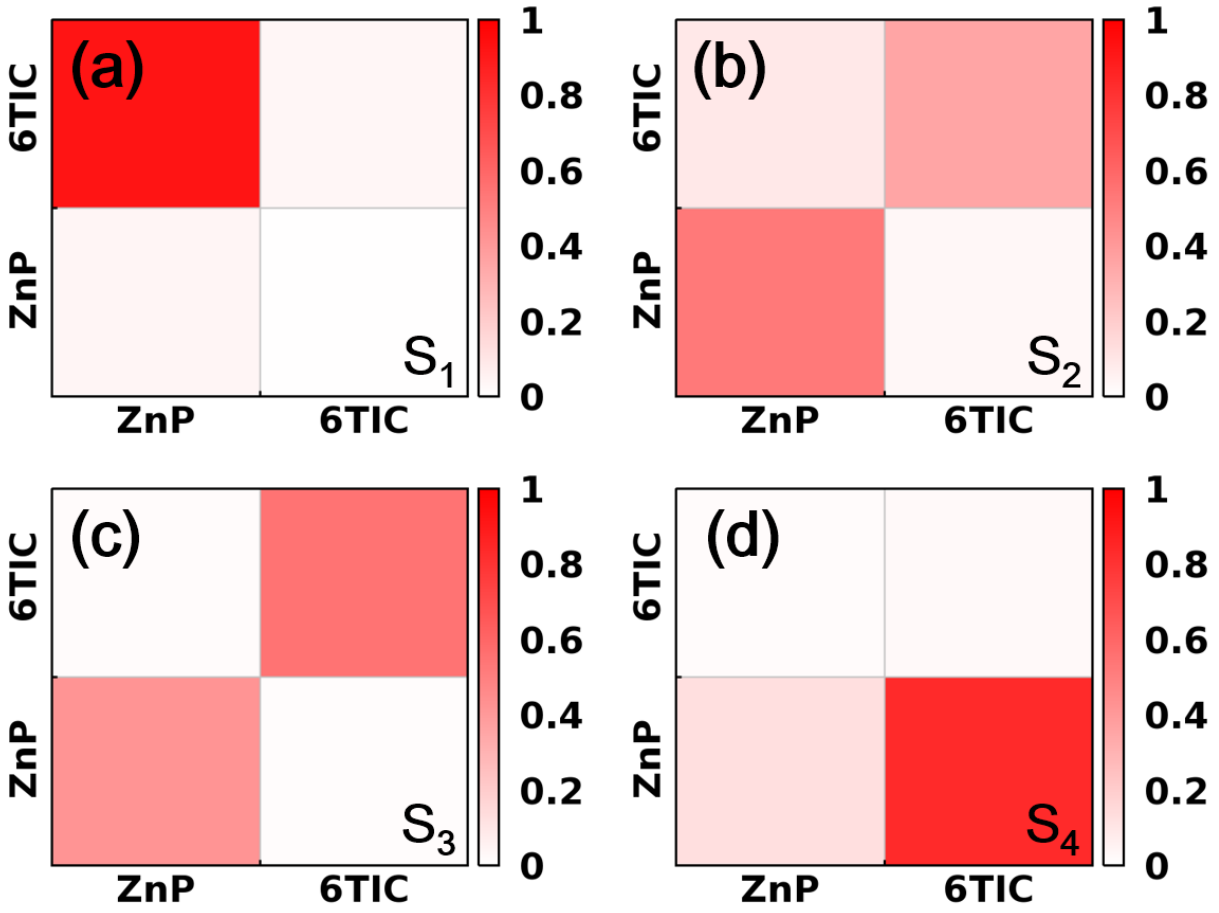

Figure S9: TD-ωB97XD* calculated one-electron transition density matrices (1TDM) for the lowest four excited states of Franck-Condon point ZnP-6TIC, where the X-axis represents the donor ZnP fragment and the Y-axis represents the acceptor 6TIC fragment.

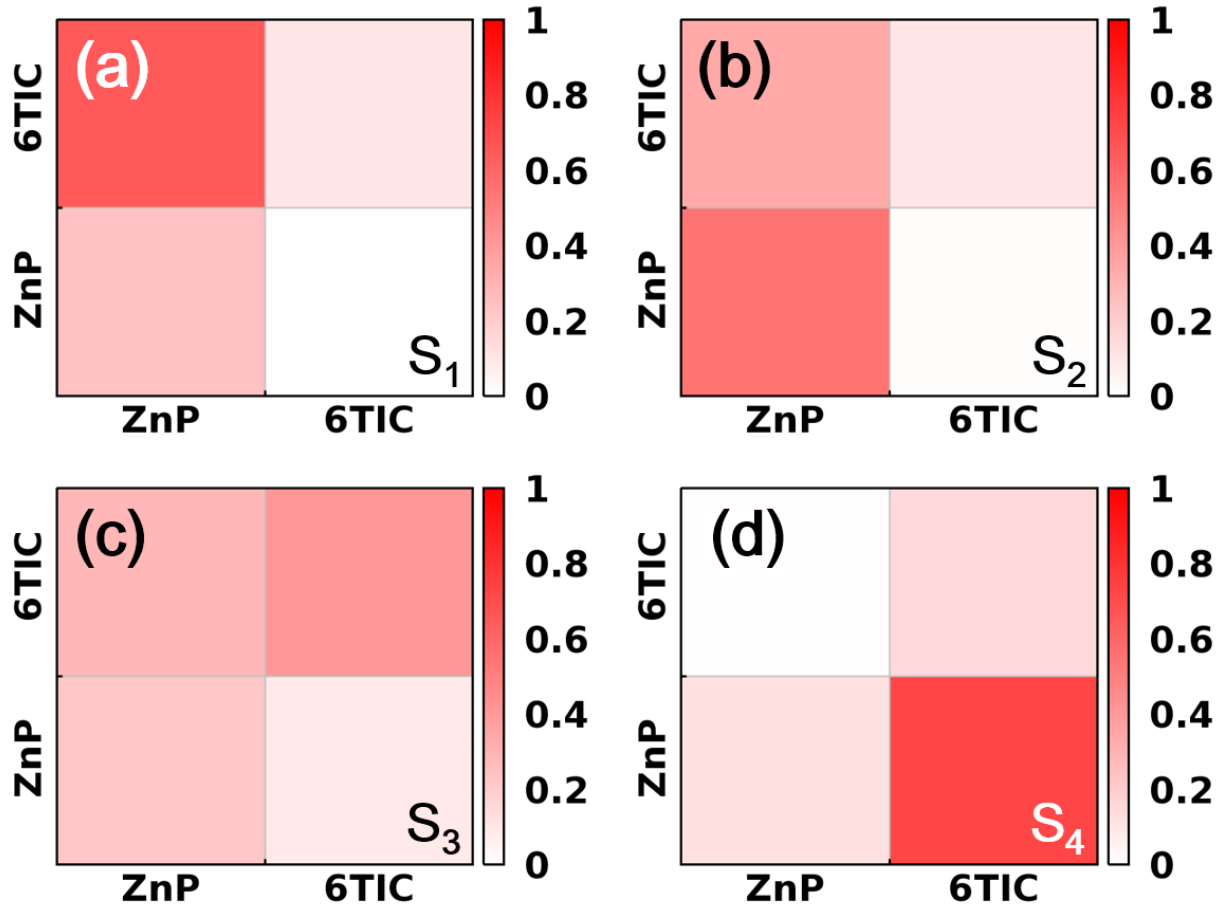

Figure S10: TD-LC-PBE0* calculated one-electron transition density matrices (1TDM) for the lowest four excited states of Franck-Condon point ZnP-6TIC, where the X-axis represents the donor ZnP fragment and the Y-axis represents the acceptor 6TIC fragment.

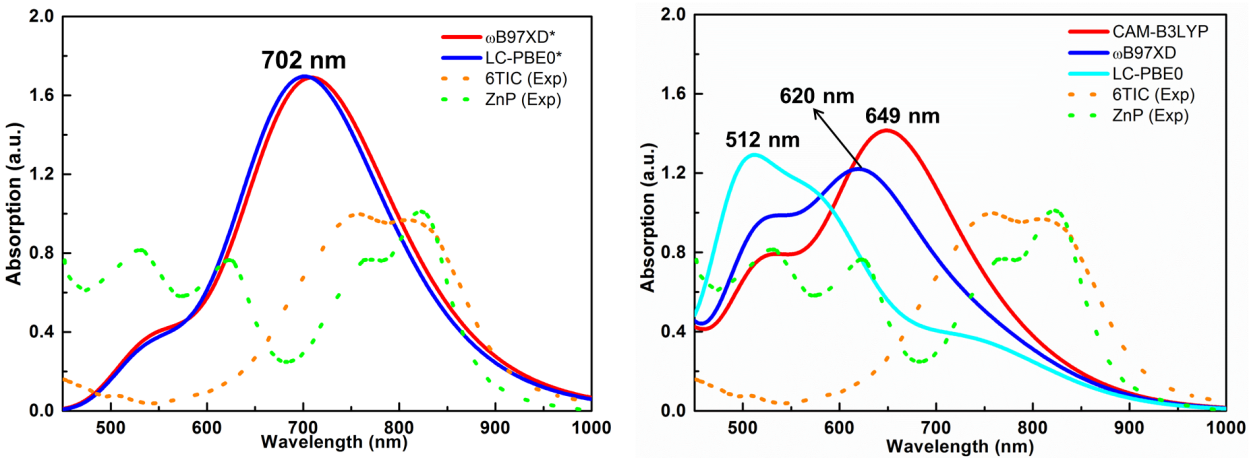

Figure S11: The absorption spectra simulated with two ORS functionals (left) and three untuned RS functionals (right). Also shown are the experimentally avaliable results for 6TIC and ZnP respectively.

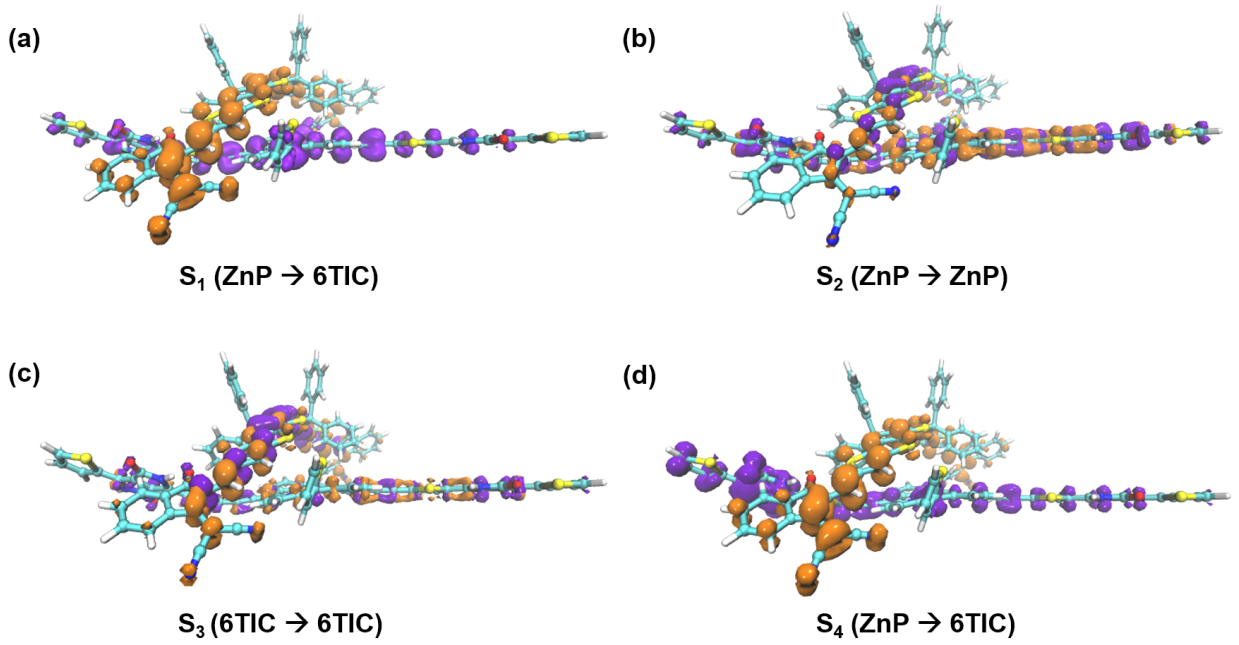

Figure S12: TD-LC-PBE0* calculated photoinduced electron (in orange) and hole (in purple) densities of the lowest four singlet excited states of ZnP-6TIC, in which the relative angle between the two molecules is ~45°. Also shown are their corresponding electronic structure characteristics roughly assigned according to their spatial distributions of electron and hole densities.

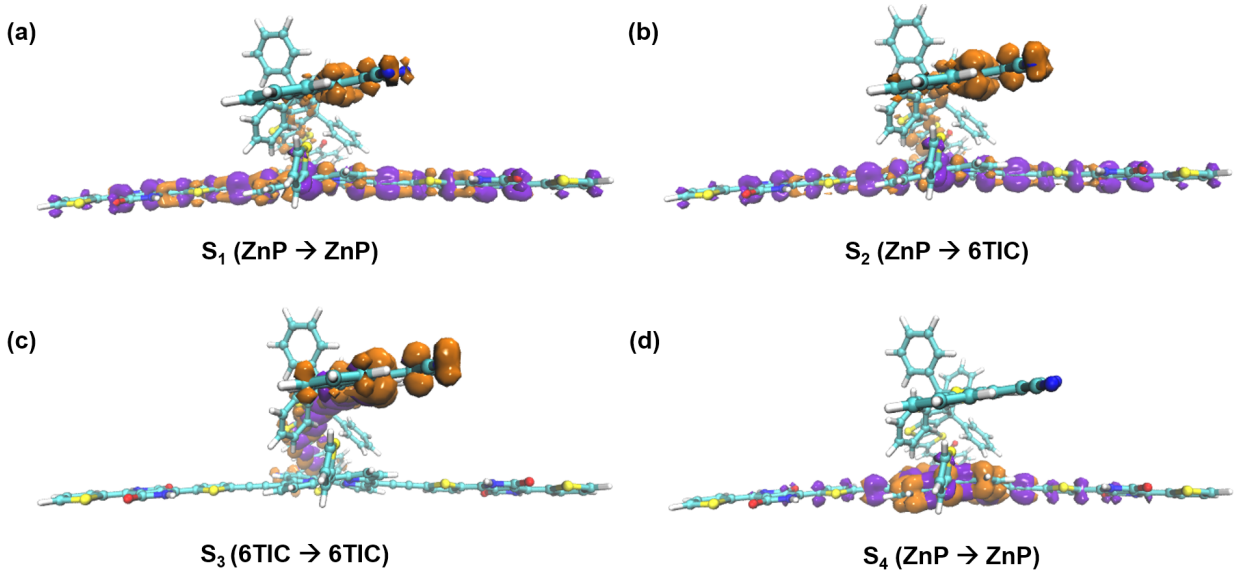

Figure S13: TD-LC-PBE0* calculated photoinduced electron (in orange) and hole (in purple) densities of the lowest four singlet excited states of ZnP-6TIC, in which the relative angle between the two molecules is ~90°. Also shown are their corresponding electronic structure characteristics roughly assigned according to their spatial distributions of electron and hole densities.

Table 1: Vertical Excitation Energies (in eV) of Lowest Lying Four Singlet Excited States Obtained Using Different Functionals.

Functionals	Vertical Excitation Energies (eV)			
	S_1	S_2	S_3	S_4
LC-PBE0*-0	1.455	1.608	1.753	1.838
LC-PBE0*-45	1.488	1.618	1.696	1.901
LC-PBE0*-90	1.603	1.606	1.730	1.981

References

(1) Barbatti, M.; Aquino, A. J. A.; Lischka, H. The UV Absorption of Nucleobases: Semi-Classical Ab Initio Spectra Simulations. *Phys. Chem. Chem. Phys.* **2010**, *12*, 4959–4967.

(2) Crespo-Otero, R.; Barbatti, M. Spectrum Simulation and Decomposition with Nuclear Ensemble: Formal Derivation and Application to Benzene, Furan and 2-Phenylfuran. *Theor. Chem. Acc.* **2012**, *131*, 1237.

(3) Liu, X.-Y.; Xie, X.-Y.; Fang, W.-H.; Cui, G. L. Photoinduced Relaxation Dynamics of Nitrogen-Capped Silicon Nanoclusters: a TD-DFT study. *Mol. Phys.* **2018**, *116*, 869–884.

(4) Liu, X.-Y.; Li, Z.-W.; Fang, W.-H.; Cui, G. L. Nonadiabatic Dynamics Simulations on Internal Conversion and Intersystem Crossing Processes in Gold(I) Compounds. *J. Chem. Phys.* **2018**, *149*, 044301.

(5) Liu, X.-Y.; Zhang, Y.-H.; Fang, W.-H.; Cui, G. L. Early-Time Excited-State Relaxation Dynamics of Iridium Compounds: Distinct Roles of Electron and Hole Transfer. *J. Chem. Phys. A* **2018**, *122*, 5518–5532.

(6) Fang, Y.-G.; Peng, L.-Y.; Liu, X.-Y.; Fang, W.-H.; Cui, G. L. QM/MM Nonadiabatic Dynamics Simulation on Ultrafast Excited-State Relaxation in Osmium(II) Compounds in Solution. *Comput. Theor. Chem.* **2019**, *1155*, 90–100.

(7) Hammes-Schiffer, S.; Tully, J. C. Proton Transfer in Solution: Molecular Dynamics with Quantum Transitions. *J. Chem. Phys.* **1994**, *101*, 4657–4667.

(8) Barbatti, M.; Aquino, A. J. A.; Szymczak, J. J.; Nachtigallová, D.; Hobza, P.; Lischka, H. Relaxation Mechanisms of UV-Photoexcited DNA and RNA Nucleobases. *Proc. Natl. Acad. Sci. U. S. A.* **2010**, *107*, 21453–21458.

(9) Lu, Y.; Lan, Z. G.; Thiel, W. Hydrogen Bonding Regulates the Monomeric Nonradiative Decay of Adenine in DNA Strands. *Angew. Chem. Int. Ed.* **2011**, *50*, 6864–6867.

(10) Long, R.; English, N. J.; Prezhdo, O. V. Photo-Induced Charge Separation across the Graphene-TiO_2 Interface Is Faster Than Energy Losses: A Time-Domain ab Initio Analysis. *J. Am. Chem. Soc.* **2012**, *134*, 14238–14248.

(11) Fazzi, D.; Barbatti, M.; Thiel, W. Unveiling the Role of Hot Charge-Transfer States in Molecular Aggregates via Nonadiabatic Dynamics. *J. Am. Chem. Soc.* **2016**, *138*, 4502–4511.

(12) Fischer, S. A.; Chapman, C. T.; Li, X. S. Surface Hopping with Ehrenfest Excited Potential. *J. Chem. Phys.* **2011**, *135*, 144102.

(13) Fischer, S. A.; Lingerfelt, D. B.; May, J. W.; Li, X. S. Non-Adiabatic Molecular Dynamics Investigation of Photoionization State Formation and Lifetime in Mn^{2+}-Doped ZnO Quantum Dots. *Phys. Chem. Chem. Phys.* **2014**, *16*, 17507–17514.

(14) Nelson, T.; Fernandez-Alberti, S.; Roitberg, A. E.; Tretiak, S. Nonadiabatic Excited-State Molecular Dynamics: Modeling Photophysics in Organic Conjugated Materials. *Acc. Chem. Res.* **2014**, *47*, 1155–1164.

(15) Richter, M.; Marquetand, P.; González-Vázquez, J.; Sola, I.; González, L. SHARC: ab Initio Molecular Dynamics with Surface Hopping in the Adiabatic Representation Including Arbitrary Couplings. *J. Chem. Theory Comput.* **2011**, *7*, 1253–1258.

(16) Richter, M.; Marquetand, P.; González-Vázquez, J.; Sola, I.; González, L. Femtosecond Intersystem Crossing in the DNA Nucleobase Cytosine. *J. Phys. Chem. Lett.* **2012**, *3*, 3090–3095.

(17) Cui, G. L.; Thiel, W. Generalized Trajectory Surface-Hopping Method for Internal Conversion and Intersystem Crossing. *J. Chem. Phys.* **2014**, *141*, 124101.

(18) Wang, Y.-T.; Liu, X.-Y.; Cui, G. L.; Fang, W.-H.; Thiel, W. Photoisomerization of Arylazopyrazole Photoswitches: Stereospecific Excited-State Relaxation. *Angew. Chem. Int. Ed.* **2016**, *55*, 14009–14013.

(19) Wang, Y.-T.; Gao, Y.-J.; Wang, Q.; Cui, G. L. Photochromic Mechanism of a Bridged Diarylethene: Combined Electronic Structure Calculations and Nonadiabatic Dynamics Simulations. *J. Phys. Chem. A* **2017**, *121*, 793–802.

(20) Xia, S.-H.; Xie, B.-B.; Fang, Q.; Cui, G. L.; Thiel, W. Excited-State Intramolecular Proton Transfer to Carbon Atoms: Nonadiabatic Surface-Hopping Dynamics Simulations. *Phys. Chem. Chem. Phys.* **2015**, *17*, 9687–9697.

(21) Xia, S.-H.; Cui, G. L.; Fang, W.-H.; Thiel, W. How Photoisomerization Drives Peptide Folding and Unfolding: Insights from QM/MM and MM Dynamics Simulations. *Angew. Chem. Int. Ed.* **2016**, *55*, 2067–2072.

(22) Zhang, Y. H.; Sun, X. W.; Zhang, T. S.; Liu, X. Y.; Cui, G. L. Nonadiabatic Dynamics Simulations on Early-Time Photochemistry of Spirobenzopyran. *J. Phys. Chem. A* **2020**, *124*, 2547–2559.

(23) Gao, Y.-J.; Chang, X.-P.; Liu, X.-Y.; Li, Q.-S.; Cui, G. L.; Thiel, W. Excited-State Decay Paths in Tetraphenylethene Derivatives. *J. Phys. Chem. A* **2017**, *121*, 2572–2579.

(24) Send, R.; Furche, F. First-Order Nonadiabatic Couplings from Time-Dependent Hybrid Density Functional Response Theory: Consistent Formalism, Implementation, and Performance. *J. Chem. Phys.* **2010**, *132*, 044107.

(25) Li, Z.; Liu, W. First-Order Nonadiabatic Coupling Matrix Elements between Excited States: A Lagrangian Formulation at the CIS, RPA, TD-HF, and TD-DFT Levels. *J. Chem. Phys.* **2014**, *141*, 014110.

(26) Li, Z.; Suo, B.; Liu, W. First Order Nonadiabatic Coupling Matrix Elements between Excited States: Implementation and Application at the TD-DFT and pp-TDA Levels. *J. Chem. Phys.* **2014**, *141*, 244105.

(27) Pittner, J.; Lischka, H.; Barbatti, M. Optimization of Mixed Quantum-Classical Dynamics: Time-Derivative Coupling Terms and Selected Couplings. *Chem. Phys.* **2009**, *356*, 147–152.

(28) Ryabinkin, I. G.; Nagesh, J.; Izmaylov, A. F. Fast Numerical Evaluation of Time-Derivative Nonadiabatic Couplings for Mixed Quantum-Classical Methods. *J. Phys. Chem. Lett.* **2015**, *6*, 4200–4203.

(29) Plasser, F.; Lischka, H. Analysis of Excitonic and Charge Transfer Interactions from Quantum Chemical Calculations. *J. Chem. Theory Comput.* **2012**, *8*, 2777–2789.

(30) Huang, J.; Du, L.; Hu, D.; Lan, Z. G. Theoretical Analysis of Excited States and Energy Transfer Mechanism in Conjugated Dendrimers. *J. Comput. Chem.* **2015**, *36*, 151–163.

(31) Lu, T.; Chen, F. Multiwfn: A Multifunctional Wavefunction Analyzer. *J. Comput. Chem.* **2012**, *33*, 580–592.

(32) Liu, Z. Y.; Lu, T.; Chen, Q. X. An Sp-Hybridized All-Carboatomic Ring, Cyclo 18 Carbon: Electronic Structure, Electronic Spectrum, and Optical Nonlinearity. *Carbon* **2020**, *165*, 461–467.

Cartesian Coordinates (in xyz format)

107

ZnP

C	-2.808744	0.474291	0.022155
C	-3.499610	1.735058	-0.078067
C	-2.536069	2.709163	-0.115864
C	-1.258284	2.038492	-0.024326
N	-1.445033	0.665370	0.050414
H	-4.581434	1.851774	-0.128654
H	-2.677092	3.783487	-0.217712
C	-0.006908	2.695866	-0.035758
C	1.247596	2.043478	-0.020670
C	2.523472	2.722752	0.021259
N	1.439204	0.668748	-0.028546
C	3.490583	1.751501	0.020594
H	2.656110	3.802279	0.060251
C	2.803973	0.484473	-0.004152
H	4.572539	1.874133	0.051621
C	-2.804058	-2.051181	0.097846
C	-3.490567	-3.318116	0.076129
C	-2.523456	-4.289398	0.082692
C	-1.247617	-3.609911	0.124743
N	-1.439305	-2.235230	0.126962
H	-4.572530	-3.439337	0.042752
H	-2.655866	-5.369120	0.048182
C	0.006975	-4.262193	0.142545

C	1.258409	-3.604998	0.126292
C	2.536640	-4.275398	0.214733
N	1.444919	-2.232069	0.047130
C	3.500063	-3.301415	0.169622
H	2.678035	-5.349441	0.319147
C	2.808783	-2.041071	0.069318
H	4.582200	-3.416447	0.215699
C	-3.463048	-0.789683	0.063060
C	3.463007	-0.777378	0.024598
C	0.006667	4.175830	-0.072215
C	0.510057	5.005120	-1.061045
S	-0.597388	5.135076	1.270602
C	0.400218	6.393664	-0.752173
H	0.932752	4.610041	-1.988119
C	-0.177161	6.619931	0.479215
H	0.730502	7.195288	-1.417176
H	-0.383651	7.573282	0.966186
C	-0.007034	-5.742004	0.185765
C	-0.509335	-6.566253	1.179326
S	0.593596	-6.708040	-1.153728
C	-0.401264	-7.956335	0.876742
H	-0.930135	-6.166460	2.105239
C	0.173620	-8.188865	-0.354636
H	-0.730993	-8.754537	1.546131
H	0.378512	-9.144663	-0.837470
Zn	-0.000024	-0.783316	0.048936
C	-4.873310	-0.790292	0.049676

C	4.873345	-0.772491	0.027731
C	6.109171	-0.774324	0.025113
C	-6.109088	-0.794594	0.041182
C	7.500447	-0.755459	0.020969
C	8.398123	-1.836945	0.046347
S	8.384813	0.773214	-0.021219
C	9.748236	-1.456008	0.032391
H	8.047699	-2.870700	0.073689
C	9.929978	-0.064340	-0.004302
H	10.603641	-2.140867	0.047127
C	-7.500332	-0.776498	0.030492
C	-8.398051	-1.858035	0.050463
S	-8.384549	0.752177	-0.014071
C	-9.748112	-1.477131	0.030498
H	-8.047769	-2.891811	0.078661
C	-9.929695	-0.085428	-0.005717
H	-10.603569	-2.162009	0.040517
C	11.178679	0.624028	-0.027374
C	12.477315	0.090432	-0.019262
C	12.693007	2.431294	-0.083380
H	10.560329	2.683615	-0.078889
C	13.413329	1.162827	-0.052815
C	13.198931	-1.175126	0.010133
C	14.710729	0.634896	-0.046274
H	15.327389	-1.424208	0.004595
C	-11.178260	0.603011	-0.033994
C	-12.476945	0.069468	-0.031960

C	-12.692193	2.410400	-0.095445
H	-10.559531	2.662568	-0.081541
C	-13.412726	1.141952	-0.068928
C	-13.198782	-1.196044	-0.006411
C	-14.710183	0.614139	-0.068299
H	-15.327223	-1.444969	-0.021676
N	11.321618	2.007613	-0.065071
N	14.566246	-0.749900	-0.008583
N	-11.320921	1.986609	-0.071291
N	-14.565969	-0.770710	-0.030604
O	13.051112	3.610057	-0.117115
C	15.992292	1.276172	-0.071010
C	17.255439	0.677192	-0.062463
S	16.141356	3.030743	-0.119640
C	18.318471	1.612835	-0.094382
H	17.407562	-0.405019	-0.034062
C	17.867694	2.920611	-0.127223
H	19.375702	1.338085	-0.093351
H	18.463258	3.833682	-0.155669
O	12.848085	-2.359977	0.043151
O	-13.050120	3.589171	-0.129931
C	-15.991569	1.255565	-0.098285
C	-17.254826	0.656737	-0.095356
S	-16.140202	3.010170	-0.147134
C	-18.317592	1.592530	-0.131708
H	-17.407196	-0.425465	-0.067743
C	-17.866501	2.900258	-0.162304

H	-19.374857	1.317922	-0.135330
H	-18.461818	3.813416	-0.193146
O	-12.848173	-2.380978	0.027375

114

6TIC

C	11.580333	-1.538354	0.074639
C	11.957637	-2.880205	0.077238
C	13.327878	-3.179359	0.096968
C	14.275919	-2.139791	0.113472
C	13.892001	-0.788070	0.111326
C	12.520235	-0.479999	0.091640
H	11.189199	-3.659325	0.064179
H	13.663958	-4.221068	0.099583
H	15.342723	-2.384491	0.128521
H	14.658840	-0.012581	0.124512
C	10.209699	-0.977109	0.054228
C	11.782650	0.810535	0.084469
C	10.352152	0.498948	0.058010
O	9.159934	-1.635508	0.036358
C	12.390134	2.068879	0.103533
C	11.673652	3.304646	0.101264
N	11.114457	4.343092	0.100449
C	13.805526	2.258198	0.129414
N	14.966822	2.459928	0.150878
C	5.446621	0.717751	-0.033817
C	5.711840	2.118303	-0.040641
C	7.070251	2.428954	-0.016896

C	7.891916	1.274288	0.009321
S	6.915535	-0.222318	0.000998
H	7.495695	3.435449	-0.017905
C	4.071480	0.429684	-0.037015
C	3.297678	1.605394	-0.056155
S	4.230699	3.081505	-0.068931
C	1.800406	-0.148336	-0.064500
C	1.913963	1.253860	-0.064863
C	-0.455051	0.549424	-0.044108
C	0.455095	-0.549366	-0.044208
S	0.381483	2.095726	-0.044514
C	-11.580378	1.538265	0.074339
C	-11.957724	2.880106	0.076757
C	-13.327976	3.179228	0.096296
C	-14.275994	2.139639	0.112780
C	-13.892040	0.787924	0.110816
C	-12.520265	0.479884	0.091349
H	-11.189304	3.659247	0.063717
H	-13.664075	4.220931	0.098753
H	-15.342807	2.384311	0.127660
H	-14.658863	0.012415	0.123963
C	-10.209730	0.977046	0.054095
C	-11.782652	-0.810639	0.084396
C	-10.352151	-0.499023	0.057959
O	-9.159977	1.635465	0.036216
C	-12.390107	-2.068996	0.103699
C	-11.673571	-3.304741	0.101620

N	–11.114354	–4.343175	0.100950
C	–13.805500	–2.258353	0.129689
N	–14.966792	–2.460109	0.151263
C	–5.446603	–0.717728	–0.033561
C	–5.711792	–2.118289	–0.040564
C	–7.070197	–2.428965	–0.017029
C	–7.891893	–1.274313	0.009241
S	–6.915526	0.222310	0.001180
H	–7.495641	–3.435462	–0.018170
C	–4.071469	–0.429608	–0.036731
C	–3.297648	–1.605305	–0.055994
S	–4.230623	–3.081450	–0.068926
C	–1.800392	0.148418	–0.064302
C	–1.913947	–1.253789	–0.064737
C	–2.790541	2.990348	1.219391
C	–2.806685	3.759900	2.389526
C	–3.324874	3.225483	3.577918
C	–3.823977	1.915944	3.586591
C	–3.803811	1.142699	2.417532
C	–3.289193	1.672968	1.221924
H	–2.409477	3.423330	0.288467
H	–2.417379	4.782901	2.368269
H	–3.343988	3.828763	4.491091
H	–4.236255	1.490089	4.507007
H	–4.192507	0.119920	2.434984
C	–4.930847	3.161832	–2.540995
C	–4.169084	2.985636	–3.705418

C	-3.065221	2.122822	-3.685037
C	-2.724584	1.436897	-2.510380
C	-3.481490	1.611318	-1.338756
C	-4.588558	2.482596	-1.365587
H	-5.797017	3.831059	-2.542997
H	-4.434078	3.520224	-4.623173
H	-2.461113	1.980195	-4.586950
H	-1.863699	0.761242	-2.506240
H	-5.176706	2.643328	-0.456247
S	-0.381457	-2.095666	-0.044551
C	-3.178344	0.814722	-0.053826
C	3.178358	-0.814644	-0.054242
C	3.289308	-1.673022	1.221402
C	2.790915	-2.990493	1.218734
C	3.803789	-1.142751	2.417072
C	2.807177	-3.760136	2.388809
H	2.409922	-3.423447	0.287767
C	3.824069	-1.916085	3.586068
H	4.192287	-0.119901	2.434627
C	3.325227	-3.225722	3.577262
H	2.418101	-4.783224	2.367459
H	4.236208	-1.490208	4.506534
H	3.344440	-3.829107	4.490363
C	3.481299	-1.611112	-1.339288
C	4.588428	-2.482339	-1.366339
C	2.724247	-1.436647	-2.510793
C	4.930616	-3.161458	-2.541828

H	5.176657	-2.643129	-0.457065
C	3.064781	-2.122480	-3.685551
H	1.863308	-0.761059	-2.506505
C	4.168685	-2.985215	-3.706146
H	5.796839	-3.830613	-2.543986
H	2.460532	-1.979824	-4.587365
H	4.433576	-3.519706	-4.623986
C	9.302807	1.410585	0.034706
H	9.587549	2.467114	0.034652
C	-9.302775	-1.410637	0.034590
H	-9.587516	-2.467168	0.034365

221

ZnP_6TIC_Parallel

C	-3.065762	-3.323201	-0.329524
C	-3.839972	-3.510972	-1.530814
C	-2.943844	-3.583508	-2.569537
C	-1.622015	-3.486473	-1.989369
N	-1.721608	-3.302524	-0.618182
H	-4.927621	-3.558256	-1.572245
H	-3.158597	-3.705339	-3.629720
C	-0.404305	-3.633274	-2.696618
C	0.875835	-3.665509	-2.089804
C	2.085590	-4.113755	-2.743973
N	1.145050	-3.339946	-0.770498
C	3.089406	-4.052184	-1.808759
H	2.149067	-4.464186	-3.772957
C	2.495426	-3.546904	-0.597005

H	4.140988	-4.313665	-1.924632
C	-2.894285	-2.721677	2.116802
C	-3.476433	-2.453083	3.408024
C	-2.485585	-1.899412	4.179880
C	-1.288386	-1.878799	3.368581
N	-1.555543	-2.402826	2.117386
H	-4.514785	-2.647145	3.671803
H	-2.543363	-1.567753	5.215469
C	-0.010788	-1.479206	3.835674
C	1.207484	-1.820363	3.204612
C	2.525859	-1.596934	3.754500
N	1.307052	-2.466993	1.981167
C	3.420465	-2.136198	2.868515
H	2.752918	-1.084403	4.685708
C	2.653034	-2.643955	1.758216
H	4.505192	-2.162967	2.948180
C	-3.624903	-3.150901	0.972347
C	3.226855	-3.181913	0.569346
C	-0.473550	-3.794871	-4.163514
C	-1.100174	-4.774601	-4.916847
S	0.270467	-2.602614	-5.221647
C	-0.977781	-4.576681	-6.324286
H	-1.610905	-5.623233	-4.455244
C	-0.265198	-3.439691	-6.642469
H	-1.394009	-5.253587	-7.074262
H	-0.019604	-3.048840	-7.630184
C	-0.002602	-0.651977	5.059644

C	–0.624193	0.579813	5.209088
S	0.756445	–1.129653	6.568880
C	–0.474929	1.141638	6.511303
H	–1.151660	1.063463	4.382487
C	0.247386	0.327523	7.359906
H	–0.885397	2.109011	6.810828
H	0.506119	0.497267	8.405444
Zn	–0.206230	–2.720591	0.631203
C	–5.010947	–3.348868	1.114548
C	4.636264	–3.171477	0.502467
C	5.857711	–2.979156	0.495825
C	–6.231707	–3.491429	1.242280
C	7.200649	–2.623590	0.578158
C	7.774775	–1.774492	1.543192
S	8.417180	–3.138698	–0.590842
C	9.140132	–1.533913	1.346953
H	7.178490	–1.340535	2.348582
C	9.661804	–2.204321	0.228337
H	9.767444	–0.884340	1.968326
C	–7.612129	–3.587157	1.372548
C	–8.394270	–3.501053	2.538297
S	–8.646842	–3.791406	–0.044667
C	–9.774670	–3.595336	2.305637
H	–7.939846	–3.376536	3.523485
C	–10.097125	–3.756140	0.948700
H	–10.555169	–3.551443	3.073814
C	11.017989	–2.148989	–0.207957

C	12.081405	-1.425749	0.361911
C	12.924889	-2.514527	-1.542847
H	10.982244	-3.277279	-2.033509
C	13.246063	-1.625422	-0.430676
C	12.390390	-0.485434	1.432592
C	14.287531	-0.842978	0.086082
H	14.225134	0.566577	1.699719
C	-11.408843	-3.874886	0.402269
C	-12.642763	-3.857638	1.071743
C	-13.104050	-4.121552	-1.218957
H	-11.011271	-4.084158	-1.701458
C	-13.685458	-4.005569	0.114096
C	-13.226765	-3.740979	2.401943
C	-14.918969	-3.989765	0.778137
H	-15.315182	-3.783566	2.880945
N	11.535123	-2.811969	-1.313861
N	13.775935	-0.208454	1.216634
N	-11.696474	-4.031137	-0.950172
N	-14.629761	-3.831933	2.131159
O	13.575777	-2.949081	-2.492741
C	15.628442	-0.634050	-0.370444
C	16.611403	0.180664	0.202973
S	16.228353	-1.388988	-1.841711
C	17.820657	0.193660	-0.532586
H	16.458717	0.743731	1.127218
C	17.758158	-0.609646	-1.659617
H	18.706183	0.766243	-0.247461

H	18.538783	-0.783156	-2.401016
O	11.720087	0.034930	2.333199
O	-13.585041	-4.261760	-2.345073
C	-16.259151	-4.104156	0.283812
C	-17.450975	-4.079270	1.014192
S	-16.591366	-4.307573	-1.434075
C	-18.605204	-4.221149	0.205786
H	-17.488109	-3.962048	2.100409
C	-18.294633	-4.353884	-1.136150
H	-19.626651	-4.226013	0.592719
H	-18.982358	-4.477486	-1.973378
O	-12.752992	-3.598802	3.534730
C	11.628394	2.440240	-0.029971
C	12.262615	3.209108	0.943545
C	13.633875	3.469636	0.788163
C	14.327344	2.963210	-0.327234
C	13.686487	2.176250	-1.300214
C	12.316922	1.901845	-1.144263
H	11.689793	3.579070	1.798949
H	14.165165	4.075013	1.530046
H	15.395263	3.173923	-0.443533
H	14.262850	1.789125	-2.141073
C	10.203699	2.028306	-0.089008
C	11.372109	1.060800	-1.924534
C	10.060660	1.174351	-1.291786
O	9.317368	2.356281	0.710803
C	11.733745	0.281542	-3.029623

C	10.863607	-0.670606	-3.641303
N	10.172660	-1.493380	-4.129488
C	13.030047	0.320066	-3.625907
N	14.083792	0.348348	-4.153784
C	5.252864	0.883032	-0.259652
C	5.282970	0.024436	-1.398363
C	6.547704	-0.115199	-1.963239
C	7.536291	0.635310	-1.281283
S	6.838672	1.534045	0.095496
H	6.794346	-0.730721	-2.831554
C	3.964673	0.989500	0.296926
C	3.036168	0.207419	-0.421623
S	3.702068	-0.640257	-1.789021
C	1.785999	1.483569	1.034418
C	1.721096	0.469708	0.064792
C	-0.537577	1.370903	0.557651
C	0.508131	2.021635	1.278776
S	0.097497	0.082692	-0.468916
C	-10.652513	4.462340	-2.930991
C	-11.224507	3.473925	-3.730294
C	-12.494211	3.718564	-4.273834
C	-13.151979	4.933459	-4.007427
C	-12.572128	5.927980	-3.201415
C	-11.300116	5.689839	-2.652005
H	-10.679891	2.542510	-3.913599
H	-12.976918	2.966193	-4.905484
H	-14.142649	5.114486	-4.436408

H	–13.116441	6.855586	–3.019827
C	–9.336263	4.436612	–2.251562
C	–10.417559	6.503979	–1.775642
C	–9.204886	5.722878	–1.525578
O	–8.518612	3.506571	–2.296022
C	–10.732769	7.780973	–1.302934
C	–9.877725	8.559293	–0.464170
N	–9.198011	9.229753	0.228445
C	–11.954620	8.453744	–1.610215
N	–12.948944	9.044806	–1.838007
C	–4.843549	4.106190	0.042945
C	–4.844519	5.362760	0.715240
C	–5.985291	6.124206	0.468706
C	–6.898458	5.469893	–0.396736
S	–6.288906	3.868120	–0.902094
H	–6.195781	7.113629	0.882021
C	–3.673722	3.367191	0.283483
C	–2.806258	4.040908	1.162375
S	–3.387346	5.602642	1.687993
C	–1.772176	2.040574	0.643163
C	–1.644341	3.238628	1.376357
C	–2.804844	0.304180	–1.934449
C	–2.502863	0.001287	–3.269031
C	–2.337158	1.031075	–4.205737
C	–2.482070	2.365957	–3.801804
C	–2.780979	2.671750	–2.466795
C	–2.942510	1.644848	–1.520759

H	-2.950871	-0.508485	-1.213687
H	-2.396649	-1.045322	-3.569933
H	-2.098952	0.791292	-5.247023
H	-2.363246	3.177105	-4.527492
H	-2.887594	3.715440	-2.154012
C	-6.370134	-0.006842	0.663524
C	-6.294456	-0.201956	2.049280
C	-5.145914	0.204880	2.741578
C	-4.086022	0.814806	2.059252
C	-4.169524	1.043894	0.675563
C	-5.319620	0.619219	-0.019330
H	-7.256304	-0.333295	0.109747
H	-7.122497	-0.682077	2.580282
H	-5.065431	0.044537	3.820793
H	-3.195202	1.131928	2.610542
H	-5.397440	0.787605	-1.097729
S	-0.051964	3.502002	2.047585
C	-3.146648	1.963359	-0.036565
C	3.244360	1.864958	1.336994
C	3.501288	3.352999	0.993283
C	4.274682	4.182155	1.822180
C	2.985127	3.878037	-0.208656
C	4.522488	5.514792	1.457455
H	4.685232	3.789988	2.756400
C	3.230653	5.206979	-0.568109
H	2.388177	3.237500	-0.867260
C	4.001359	6.032339	0.265792

H	5.128652	6.146980	2.114319
H	2.818863	5.598969	-1.503755
H	4.194246	7.072611	-0.015216
C	3.623983	1.535905	2.793668
C	4.875204	0.979944	3.115352
C	2.745679	1.854111	3.846220
C	5.242260	0.758787	4.450872
H	5.576795	0.710592	2.322698
C	3.104895	1.627214	5.180966
H	1.757274	2.269191	3.636853
C	4.359132	1.081086	5.490385
H	6.225552	0.331178	4.674192
H	2.388365	1.860594	5.974933
H	4.642248	0.902545	6.532662
C	8.876499	0.600103	-1.737553
H	8.956160	-0.016930	-2.637259
C	-8.120902	6.099854	-0.740419
H	-8.193282	7.083923	-0.267539

221

ZnP_6TIC_Perpendicular

C	2.861370	-0.193358	-2.250884
C	3.750930	-1.324881	-2.163997
C	2.960529	-2.445922	-2.123282
C	1.588144	-1.994222	-2.202616
N	1.548950	-0.608722	-2.240707

H	4.838796	–1.264342	–2.160093
H	3.274808	–3.487942	–2.095100
C	0.476061	–2.847789	–2.388315
C	–0.840004	–2.397450	–2.665215
C	–1.970577	–3.249715	–2.953958
N	–1.259999	–1.078548	–2.562057
C	–3.081323	–2.442581	–2.995712
H	–1.922512	–4.330933	–3.067622
C	–2.631816	–1.105170	–2.698615
H	–4.119149	–2.729525	–3.162596
C	2.409455	2.286899	–2.439453
C	2.834723	3.653023	–2.607119
C	1.722846	4.437449	–2.417750
C	0.621663	3.546442	–2.130441
N	1.054216	2.230984	–2.198266
H	3.853193	3.966670	–2.833572
H	1.651869	5.521987	–2.471834
C	–0.692152	3.951858	–1.776300
C	–1.794342	3.066180	–1.681603
C	–3.141618	3.437851	–1.311261
N	–1.759807	1.725045	–2.038793
C	–3.932608	2.334872	–1.525126
H	–3.446470	4.410549	–0.929367
C	–3.062876	1.285522	–1.991004
H	–5.007208	2.235703	–1.376302
C	3.283986	1.159498	–2.404709
C	–3.497061	–0.013326	–2.392120

C	0.682356	–4.303095	–2.219806
C	0.519734	–5.343408	–3.120269
S	1.080163	–4.933242	–0.628792
C	0.718000	–6.631238	–2.536790
H	0.278193	–5.173800	–4.172877
C	1.024803	–6.569001	–1.192805
H	0.637739	–7.569912	–3.090660
H	1.192746	–7.383716	–0.486722
C	–0.888110	5.388119	–1.510802
C	–0.147006	6.190154	–0.653404
S	–2.077890	6.363663	–2.369143
C	–0.530670	7.561019	–0.678708
H	0.632693	5.781669	–0.006853
C	–1.559908	7.808616	–1.563939
H	–0.081965	8.326436	–0.042562
H	–2.058489	8.755158	–1.775074
Zn	–0.105640	0.567033	–2.262406
C	4.666780	1.408467	–2.512067
C	–4.885311	–0.250053	–2.435298
C	–6.105275	–0.447010	–2.463566
C	5.875122	1.653686	–2.600345
C	–7.475539	–0.683935	–2.493071
C	–8.530668	0.220508	–2.280092
S	–8.110973	–2.299490	–2.822239
C	–9.804447	–0.358674	–2.377103
H	–8.345690	1.274712	–2.064084
C	–9.767269	–1.731507	–2.669836

H	-10.755927	0.169455	-2.247433
C	7.234847	1.929589	-2.699665
C	7.869301	3.180063	-2.804690
S	8.433866	0.632228	-2.708359
C	9.267053	3.103665	-2.888439
H	7.299175	4.111239	-2.817956
C	9.751940	1.786477	-2.849472
H	9.948085	3.957941	-2.975557
C	-10.894464	-2.589816	-2.832012
C	-12.259043	-2.273759	-2.736197
C	-12.115200	-4.567789	-3.232647
H	-9.969129	-4.483369	-3.262317
C	-13.020061	-3.452785	-2.974625
C	-13.165705	-1.162191	-2.477745
C	-14.382877	-3.141899	-2.880363
H	-15.307053	-1.247601	-2.457260
C	11.120817	1.392279	-2.915063
C	12.261718	2.203191	-3.028099
C	13.003200	-0.027580	-2.966000
H	10.987661	-0.751857	-2.803043
C	13.414632	1.369028	-3.061378
C	12.675957	3.597257	-3.123935
C	14.555671	2.173511	-3.175669
H	14.687459	4.316042	-3.293231
N	-10.824463	-3.948511	-3.124439
N	-14.451766	-1.782733	-2.585259
N	11.573777	0.077394	-2.878344

N	14.100790	3.489491	-3.210833
O	-12.290375	-5.761166	-3.486077
C	-15.550555	-3.958336	-3.034008
C	-16.890268	-3.574458	-2.922405
S	-15.428956	-5.674438	-3.412354
C	-17.797188	-4.640845	-3.137653
H	-17.205822	-2.553491	-2.691999
C	-17.151356	-5.833466	-3.412324
H	-18.883797	-4.538631	-3.093058
H	-17.600071	-6.806219	-3.616395
O	-12.999720	0.035547	-2.222304
O	13.620008	-1.094155	-2.953598
C	15.946494	1.836299	-3.249402
C	17.037427	2.703318	-3.363043
S	16.490870	0.161626	-3.200827
C	18.283235	2.031275	-3.409701
H	16.938934	3.791034	-3.410949
C	18.142890	0.656795	-3.331750
H	19.248021	2.535937	-3.497257
H	18.929495	-0.098389	-3.344852
O	12.066008	4.672562	-3.137584
C	1.979600	-10.999434	0.949728
C	0.826926	-11.720557	0.641859
C	0.973803	-13.054722	0.233824
C	2.255998	-13.626456	0.142879
C	3.416180	-12.895653	0.451841
C	3.277331	-11.558650	0.862683

H	-0.152589	-11.239676	0.726277
H	0.092512	-13.654654	-0.014079
H	2.359266	-14.668116	-0.177123
H	4.391521	-13.376353	0.366043
C	2.082522	-9.593674	1.402430
C	4.267540	-10.522599	1.257579
C	3.522277	-9.307890	1.592498
O	1.128694	-8.812808	1.557338
C	5.649437	-10.724075	1.299336
C	6.592851	-9.726409	1.693553
N	7.398954	-8.926846	2.012697
C	6.273708	-11.960770	0.951740
N	6.828865	-12.962771	0.673402
C	2.200905	-4.817751	3.096666
C	3.611836	-4.611633	3.043426
C	4.328727	-5.741106	2.656357
C	3.489874	-6.848434	2.373926
S	1.766410	-6.438957	2.617273
H	5.415249	-5.805661	2.559535
C	1.500462	-3.656211	3.458627
C	2.375011	-2.570064	3.664356
S	4.064308	-2.952808	3.445070
C	0.240678	-1.715834	3.824741
C	1.607999	-1.391165	3.904342
C	0.201956	0.641013	3.985912
C	-0.558135	-0.561703	3.862742
S	1.928375	0.317240	4.087402

C	–1.663980	11.303383	1.348923
C	–0.558769	12.104147	1.632501
C	–0.587038	13.441205	1.208371
C	–1.708343	13.938279	0.519486
C	–2.820423	13.127562	0.233402
C	–2.798939	11.786602	0.653978
H	0.293756	11.680619	2.172632
H	0.261731	14.101424	1.412710
H	–1.721045	14.983627	0.195129
H	–3.670206	13.552170	–0.302649
C	–1.869435	9.875827	1.689032
C	–3.777111	10.675598	0.514072
C	–3.205571	9.501447	1.173293
O	–1.057369	9.151645	2.285386
C	–4.994916	10.774556	–0.165609
C	–5.910751	9.690525	–0.329473
N	–6.686740	8.816444	–0.487576
C	–5.453220	11.976900	–0.785169
N	–5.868455	12.947563	–1.309801
C	–2.308890	4.944195	2.767688
C	–3.643714	4.738695	2.304385
C	–4.233610	5.887528	1.784193
C	–3.372194	7.013881	1.838619
S	–1.800736	6.600180	2.578547
H	–5.237113	5.954299	1.356551
C	–1.716136	3.762109	3.237741
C	–2.598990	2.668432	3.140809

S	-4.165168	3.060973	2.478702
C	-0.569831	1.799801	3.804322
C	-1.910451	1.477966	3.519994
C	1.188351	3.555032	5.780630
C	1.446079	3.906858	7.110207
C	0.439021	4.492185	7.892644
C	-0.824026	4.721166	7.332501
C	-1.084804	4.364584	6.001122
C	-0.081601	3.777897	5.211928
H	1.988341	3.122853	5.170440
H	2.439191	3.726022	7.533915
H	0.641183	4.772487	8.931295
H	-1.615751	5.184498	7.930039
H	-2.075001	4.548737	5.574437
C	2.391879	5.433914	2.092035
C	2.838148	4.583591	1.069164
C	2.234012	3.330507	0.898186
C	1.197081	2.924319	1.747823
C	0.769847	3.754189	2.799874
C	1.367631	5.020214	2.954688
H	2.845230	6.421021	2.228889
H	3.643222	4.896133	0.397039
H	2.568119	2.663014	0.099982
H	0.725379	1.949031	1.592555
H	1.046745	5.675985	3.770300
S	-2.257829	-0.233616	3.545797
C	-0.348862	3.315948	3.759547

C	0.045760	–3.226794	3.656378
C	–0.548736	–3.751886	4.988308
C	–1.923863	–3.573883	5.238864
C	0.249753	–4.350854	5.976724
C	–2.485362	–3.982623	6.453700
H	–2.563412	–3.133002	4.467155
C	–0.315513	–4.765036	7.191975
H	1.318398	–4.500824	5.797996
C	–1.682254	–4.581029	7.436367
H	–3.556036	–3.836969	6.629754
H	0.320416	–5.237978	7.947313
H	–2.122153	–4.906528	8.384419
C	–0.831158	–3.618747	2.458552
C	–1.361579	–4.921664	2.383841
C	–1.126436	–2.705529	1.432590
C	–2.183291	–5.294541	1.312863
H	–1.152201	–5.639829	3.183527
C	–1.984313	–3.065902	0.385903
H	–0.697266	–1.699824	1.450355
C	–2.513473	–4.360669	0.320449
H	–2.576554	–6.314912	1.266010
H	–2.239995	–2.325533	–0.374837
H	–3.174488	–4.637280	–0.506323
C	4.059171	–8.082589	1.975886
H	5.151648	–8.022114	1.981602
C	–3.799873	8.249356	1.297109
H	–4.810651	8.160063	0.888421